PROCEEDINGS OF SCIENCE

Electromagnetic splitting of charged and neutral mesons

Aaron Torok*

E-mail: amtorok@indiana.edu

S. Basak[b], A. Bazavov[c], C. Bernard[d], C. DeTar[e], E. Freeland[f], W. Freeman[c], Steven Gottlieb[a,g], U.M. Heller[h], J.E. Hetrick[i], Volodymyr Kindratenko[g], J. Laiho[j], L. Levkova[e], M. Oktay[e], J. Osborn[k], Guochun Shi[g], R.L. Sugar[l], D. Toussaint[c], R.S. Van de Water[m]

[a] Department of Physics, Indiana University, Bloomington, IN 47405, USA
[b] School of Physical Sciences, NISER, Bhubaneswar, Orissa 751005, India
[c] Department of Physics, University of Arizona, Tucson, AZ 85721, USA
[d] Department of Physics, Washington University, St. Louis, MO 63130, USA
[e] Physics Department, University of Utah, Salt Lake City, UT 84112, USA
[f] Department of Physics, University of Illinois, Urbana, IL 61801, USA
[g] NCSA, University of Illinois, Urbana, IL 61801, USA
[h] American Physical Society, One Research Road, Ridge, NY 11961, USA
[i] Physics Department, University of the Pacific, Stockton, CA 95211, USA
[j] SUPA, School of Physics and Astronomy, University of Glasgow, Glasgow G12 8QQ, UK
[k] ALCF, Argonne National Laboratory, Argonne, IL 60439, USA
[l] Department of Physics, University of California, Santa Barbara, CA 93106, USA
[m] Department of Physics, Brookhaven National Laboratory, Upton, NY 11973, USA

We extend MILC's initial study of the electromagnetic splitting of charged and neutral mesons, and the violation of Dashen's theorem. Meson masses are calculated using the MILC $N_f = 2+1$, asqtad $SU(3)$ gauge configurations, and independently generated $U(1)$ gauge configurations. The meson correlators are calculated using $SU(3) \times U(1)$ gauge fields. A large fraction of the meson correlators are calculated using an implementation of the MILC staggered multi-mass inverter that runs on a single NVIDIA GPU in double precision. When the current analysis is complete, we will have results at three lattice spacings, from about 0.15 to 0.09 fm, with several light quark masses at each lattice spacing. Once electromagnetic effects are included in the corresponding rooted, staggered chiral perturbation theory calculations, we should have excellent control over the chiral and continuum limits.

The XXVIII International Symposium on Lattice Field Theory, Lattice2010
June 14-19, 2010
Villasimius, Italy

*Speaker.

PoS(Lattice 2010)127

1. Introduction

With increasing computational power, the inclusion of electromagnetic effects in Lattice QCD calculations is becoming necessary to achieve $< 1\%$ precision. The systematic error due to electromagnetic effects can be significant. For instance, MILC calculated the light quark mass ratio,

$$m_u/m_d = 0.42(0)(1)(4),$$

where the errors are statistical, lattice-systematic, and electromagnetic (from continuum estimates) [1, 2]. This $SU(3) \times U(1)$ calculation eliminates the need for an estimate of the error from continuum phenomenology, as lattice statistical errors and systematics will be quantified. Also, MILC points out that the calculation of m_u/m_d rules out the possibility of the u quark being massless at the 10σ-level [2], which is important with regard to the strong CP problem. Fully quantifying the uncertainty in m_u/m_d from the lattice could strengthen this point.

This work is an extension of the initial MILC study that was done with the MILC gauge ensembles with lattice spacing $a \approx 0.15$ fm [3]. Almost all of the lattice studies of $SU(3) \times U(1)$ to date have used a quenched $U(1)$ gauge field generated in momentum space, gauge-fixed and Fourier transformed to coordinate space [4, 5, 6]. One benefit of this approach is that the $U(1)$ gauge fields have no, or minimal, autocorrelations due to the fact that the fields are generated in momentum space randomly. Additionally, most $SU(3) \times U(1)$ studies to date, including this one, consider the isospin-symmetric case, with the u and d quark of degenerate mass. Recently, however, there was a study which considered explicit isospin breaking in addition to electromagnetic (EM) effects [7, 8].

The eventual goal of this program is to systematically include dynamical EM effects in the gauge field generation, *i.e.*, dynamical $U(1)$. A fully dynamical calculation of $SU(3) \times U(1)$ is more difficult because the molecular dynamics equations that are solved have some terms that depend on the charge of each quark that is considered. This complicates the fermion force calculation, which is the most costly part of the gauge field generation. Another factor is that there are not $2+1$ flavors anymore, but 3 since the u and d quarks still have degenerate mass, but different charges.

2. Methodology

The MILC $N_f = 2+1$, asqtad $SU(3)$ gauge configurations were used, and separately generated $U(1)$ gauge fields multiply each $SU(3)$ link to obtain a $SU(3) \times U(1)$ gauge field. The $U(1)$ gauge field is fattened in the same way as the SU(3). The reason for this is that the current version of the code globally multiplies each $SU(3)$ link by the $U(1)$ link before the link fattening occurs. The CPU code computation is dominated by the Conjugate Gradient (CG) operation which occurs during the propagator generation. Due to this fact, we realized that the quenched QED code was a particularly good candidate for implementation in GPUs due to the parallel development of a staggered, GPU based CG inverter by Guochun Shi [9]. Additionally, it turns out that the $a \approx 0.12$ fm lattices were small enough to fit into the device memory of one GPU, and into the host memory on one node of all of the GPU clusters that we had access to. The $a \approx 0.09$ fm, $28^3 \times 96$ lattices fit on one node at Fermilab (FNAL), due to a relatively large amount of host memory on the Jpsi nodes.

Machine	t (h)	size	cpu cores	gpu	nodes	core-hr	node-hr
Big Red	13.3	$28^3 \times 96$	32	none	8	426	106.4
Jpsi at FNAL	7.8	$28^3 \times 96$	1	S1070	1	7.8	7.8
Jpsi at FNAL	0.8	$20^3 \times 64$	64	none	8	51.2	6.4
AC at NCSA	1.5	$20^3 \times 64$	1	S1070	1	1.5	1.5

Table 1: A comparison of the CPU code *vs.* GPU code for two lattice spacings. The CG acceleration by the GPU is impressive, but the acceleration on a node is dependent on the hardware configuration, and machine-dependent.

The quenched $U(1)$ gauge field generation time is small compared with the $SU(3)$ generation. The $U(1)$ gauge generation code is a serial code, and only requires a few minutes per configuration on a scalar machine (up to $28^3 \times 96$ lattices). As the configurations get bigger, each $U(1)$ gauge field could require on the order of a few core-hours. If the quenched QED $U(1)$ lattice generation is to be used on lattices much larger than $48^3 \times 144$, it is possible that the code will have to be parallelized.

2.1 GPU Implementation

GPUs are becoming more common in scientific computation, and there are now several clusters with GPU-enhanced nodes. The general idea of these hybrid architectures is that the GPU operates as an accelerator for the computationally intensive operations. NVIDIA has developed the CUDA language that facilitates GPU programming using the C language. Also, QUDA [10] has been developed recently which is specific to Lattice QCD.

The calculation of the electromagnetic contribution to the meson masses is particularly well suited for the GPU since in this calculation the CPU code spends almost all of its time in the CG routine. The staggered CG inverter code, written by Guochun Shi, speeds up the CG operation considerably [11]. The GPU itself is composed of several hundred streaming cores. A single CPU core has exclusive access to a GPU. Not all CPU cores on a compute node are mated to a GPU, which is a consideration for multi-GPU code. The code used for these calculations utilized only one GPU and one CPU core per compute node.

Table 1 shows the timing data for typical runs of the CPU code and the GPU code. The runs on Big Red were CPU-only runs, while the runs at FNAL and at the NCSA used GPUs. There is a large speedup when comparing node-hours for the CPU *vs.* GPU code, and this is expected to improve in the case of multi-GPU code. The increase in performance will be machine-dependent as some clusters have one GPU per node, and others have two.

3. Dashen's Theorem and χPT

Dashen's Theorem is the statement that, to Leading Order (LO), the electromagnetic contribution to the double difference,

$$\Delta M_D^2 = (m_{K^+}^2 - m_{K^0}^2) - (m_{\pi^+}^2 - m_{\pi^0}^2), \tag{3.1}$$

is equal to zero. The χPT for the electromagnetic contribution to the pion and kaon masses was developed in Ref. [12], and for partially-quenched χPT in Ref. [13]. The staggered χPT was recently constructed [14], and an extrapolation to the physical point using the data from this study is forthcoming. The LO electromagnetic contribution to the meson masses is,

$$\chi_{e,ij} = \chi_{ij} + \frac{2Ce^2}{F_0^2}(q_i - q_j)^2 . \tag{3.2}$$

In the notation of Bijnens and Danielsson [13], $\chi_{e,ij}$ is m^2_{meson}, with $e \neq 0$, and χ_{ij} is m^2_{meson}, with $e = 0$. C is a low energy constant, q_i and q_j are the charges on the valence quark and anti-quark, F_0 is the decay constant in the chiral limit, and e is the electric charge. The LO contribution disappears in the difference,

$$\begin{aligned} \Delta M^2_{D\chi} \;=\; & M^2(\chi_1,\chi_3,q_1,q_3) - M^2(\chi_1,\chi_3,q_3,q_3) \\ & - M^2(\chi_1,\chi_1,q_1,q_3) + M^2(\chi_1,\chi_1,q_3,q_3), \end{aligned} \tag{3.3}$$

where,

$$\begin{aligned} m^2_{K^+} - m^2_{K^0} &= M^2(\chi_1,\chi_3,q_1,q_3) - M^2(\chi_1,\chi_3,q_3,q_3) \\ m^2_{\pi^+} - m^2_{d\bar{d}} &= M^2(\chi_1,\chi_1,q_1,q_3) - M^2(\chi_1,\chi_1,q_3,q_3). \end{aligned} \tag{3.4}$$

Reference [13] points out that $\Delta M^2_{D\chi}$ becomes ΔM^2_D up to very small corrections to m_{π^0}. Therefore, the difference $\Delta M^2 \equiv \chi_{e,ij} - \chi_{ij}$ measures the LO electromagnetic correction, and $\Delta M^2_{D\chi}$ measures the NLO correction. In this case, $m_{d\bar{d}}$ is the meson that is treated like the π^0. In addition, the measure of higher order corrections to Dashen's Theorem can be parameterized as [1]

$$\Delta E = \frac{M^2(\chi_1,\chi_3,q_1,q_3) - M^2(\chi_1,\chi_3,q_3,q_3)}{M^2(\chi_1,\chi_1,q_1,q_3) - M^2(\chi_1,\chi_1,q_3,q_3)} - 1. \tag{3.5}$$

If $\Delta E \neq 0$ then Dashen's Theorem is violated, and there is evidence of NLO effects. Reference [13] also points out that $\Delta M^2_{D\chi}$, or equivalently, ΔE may be calculated with controlled errors with *quenched* EM. Recently, Freeland and Bernard developed the staggered χPT for the mesons with EM effects [14]. The lattice-spacing effects are expected to reduce to $a^2 q^2_{ij}$ and $a^2(q_i^2 - q_j^2)$ at NLO, with no sea quark term at $\mathcal{O}(a^2)$ in the mass-squared differences.

4. Data and Results

In this study, we used two values of $\alpha_{\rm EM}$. Since this is a tunable parameter in the calculation, we are free to change e, providing more data points for the chiral fits. We use $e = 0.303$, and $e = 0.606$, corresponding to $\alpha_{\rm phys}$, and $4\alpha_{\rm phys}$, respectively. In addition, Blum *et al.*, found that averaging over $\pm e$ provides a cancellation of $\mathcal{O}(e)$ noise which can be significant when calculating mass-squared differences [6]. This effect is shown in Fig. 1 for $\alpha_{\rm phys}$. The other expected benefit illustrated in Fig. 3, is that there will be a higher signal to noise ratio as the strength of $\alpha_{\rm EM}$ increases. This may prove to be useful for the chiral fits, and from the data in Fig. 3, it is clear that ΔE, or equivalently, Dashen's violation is small, but significantly different from zero. The statistics that we have accumulated are in Table 2.

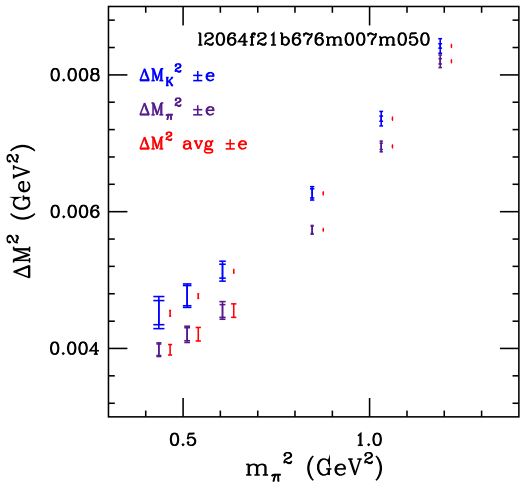

Figure 1: The mass-squared differences with no averaging over $\pm e$, and with averaging. Only the error bars are shown, the central value is omitted.

ensemble	m_l/m_s	a (fm)	cfgs
l2064f21b676m007m050	0.14	0.12	1261
l2464f21b676m005m050	0.1	0.12	1274
l2896f21b709m0062m031	0.2	0.09	331
l2896f21b711m0124m031	0.4	0.09	331

Table 2: The statistics we have for the $SU(3) \times U(1)$ calculation.

5. Conclusions

The mass-squared differences of the charged and neutral mesons that we calculated in this extended study show noise cancellation when averaging over $\pm e$, and also, when forming the ratio ΔE there is an increased signal to noise ratio due to the doubling of e, or $\alpha_{\rm EM} \to 4\alpha_{\rm EM}$. Additionally, ΔM_π^2 or ΔM_K^2 represents the LO electromagnetic contribution, whereas $\Delta M_{D\chi}^2$ represents the NLO contribution. The magnitude of these contributions are in accordance with a perturbative effect, and are on the order of what one would expect from a physical estimate based on the electromagnetic contribution to the physical pion mass.

Based on these facts and also future calculations at another lattice spacing 0.06 fm, and possibly 0.045 fm, as well as at least one other volume, we should have excellent control over the chiral, and continuum limits in this calculation. The staggered χPT has been constructed [14], and the physical extrapolation is forthcoming. This will complete the extension of this project with regard to the meson mass-squared differences for quenched, non-compact QED. Subsequently, fully dynamical $SU(3) \times U(1)$ fields need to be implemented to quantify the interactions of charged sea quarks, which may become more important for studying the electromagnetic effects on the baryon masses.

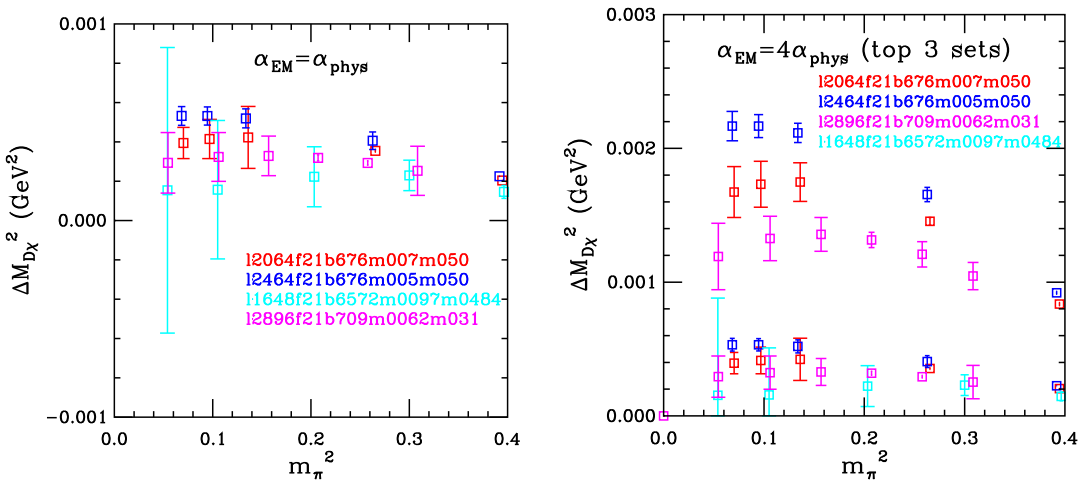

(a) (b)

Figure 2: The difference $\Delta M_{D\chi}^2$ for four MILC ensembles, at two values of $\alpha_{\rm EM}$. In (b), the $a = 0.15$ fm data was not calculated for $4\alpha_{\rm phys}$.

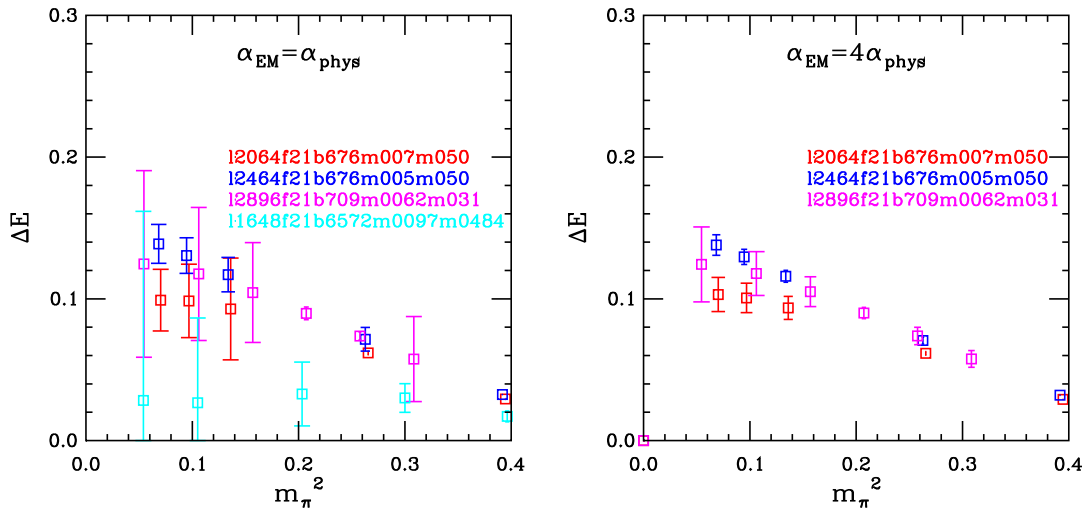

(a) (b)

Figure 3: The difference ΔE for four MILC ensembles, at two values of $\alpha_{\rm EM}$. In (b), the $a = 0.15$ fm data was not calculated for $4\alpha_{\rm phys}$.

Acknowledgements

A.T. is grateful for the hospitality of NCSA while this work was carried out. We would like to thank Michael Clark from Harvard University, Ronald Babich from Boston University, and Balint Joo from Jefferson Lab for code sharing and helpful discussions. This work was partially supported by NSF grant PHY-0555234 and the Institute for Advanced Computing Applications and Technologies (IACAT) at the University of Illinois at Urbana-Champaign. This work was in part based on the MILC collaboration's public lattice gauge theory code. This research used resources of the National Energy Research Scientific Computing Center, which is supported by the Office of

Science of the U.S. Department of Energy under Contract No. DE-AC02-05CH11231.

References

[1] C. Aubin et al. Light pseudoscalar decay constants, quark masses, and low energy constants from three-flavor lattice QCD. *Phys. Rev.*, D70:114501, 2004.

[2] A. Bazavov et al. Full nonperturbative QCD simulations with 2+1 flavors of improved staggered quarks. *Rev. Mod. Phys.*, 82:1349–1417, 2010.

[3] S. Basak et al. Electromagnetic splittings of hadrons from improved staggered quarks in full QCD. *PoS*, LATTICE2008:127, 2008.

[4] A. Duncan, E. Eichten, and H. Thacker. Electromagnetic splittings and light quark masses in lattice QCD. *Phys. Rev. Lett.*, 76:3894–3897, 1996.

[5] A. Duncan, E. Eichten, and H. Thacker. Electromagnetic structure of light baryons in lattice QCD. *Phys. Lett.*, B409:387–392, 1997.

[6] Thomas Blum, Takumi Doi, Masashi Hayakawa, Taku Izubuchi, and Norikazu Yamada. Determination of light quark masses from the electromagnetic splitting of pseudoscalar meson masses computed with two flavors of domain wall fermions. *Phys. Rev.*, D76:114508, 2007.

[7] T. Blum, R. Zhou, T. Doi, M. Hayakawa, T. Izubuchi, et al. Electromagnetic mass splittings of the low lying hadrons and quark masses from 2+1 flavor lattice QCD+QED. 2010.

[8] Taku Izubuchi. Studies of the QCD and QED effects on isospin breaking. *PoS*, KAON09:034, 2009.

[9] G. Shi, S. Gottlieb, A. Torok, and V. Kindratenko. Accelerating quantum chromodynamics calculations with gpus. In *Proc. Symposium on Application Accelerators in HPC (SAAHPC10)*, Knoxville, TN, July 2010.

[10] M. A. Clark, R. Babich, K. Barros, R. C. Brower, and C. Rebbi. Solving Lattice QCD systems of equations using mixed precision solvers on GPUs. *Comput. Phys. Commun.*, 181:1517–1528, 2010.

[11] S. Gottlieb, G. Shi, A. Torok, and V. Kindratenko. Quda programming for staggered quarks. In *Proc. XXVIII International Symposium on Lattice Field Theory (Lattice 2010)*, Villasimius, Sardinia, June 2010.

[12] P. Langacker and H. Pagels. Pion and kaon electromagnetic masses in chiral perturbation theory. *Phys. Rev.*, D8:4620–4627, 1973.

[13] Johan Bijnens and Niclas Danielsson. Electromagnetic Corrections in Partially Quenched Chiral Perturbation Theory. *Phys. Rev.*, D75:014505, 2007.

[14] E. Freeland and C. Bernard. Progress in electromagnetic corrections to staggered chiral perturbation theory. In *Proc. XXVIII International Symposium on Lattice Field Theory (Lattice 2010)*, Villasimius, Sardinia, June 2010.